Thermal Science and Engineering Progress 63 (2025) 103721

Contents lists available at ScienceDirect

Thermal Science and Engineering Progress

journal homepage: www.sciencedirect.com/journal/thermal-science-and-engineering-progress

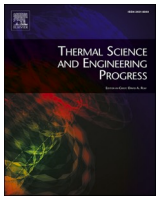

Energy storage using direct iron oxide reduction and energy utilization with high temperature metal combustion☆

Luis M. Romeo [a,b,*], Javier Saez-Guinoa [a,b], Santiago Jiménez [c], Carmen Mayoral [b,c]

[a] Aragon Institute of Engineering Research (I3A), Universidad de Zaragoza, Department of Mechanical Engineering, Zaragoza 50018, Spain
[b] Energy and CO2 Research Group, Spain
[c] Instituto de Carboquímica-CSIC, Miguel Luesma 4, 50018 Zaragoza, Spain

A B S T R A C T

In response to the growing demand for renewable energy storage solutions, metal fuels have emerged as a promising alternative as recyclable energy carriers. These metals release energy through combustion, forming metal oxides, which can subsequently be regenerated into their metallic state using renewable hydrogen. Recent experimental studies have demonstrated the feasibility of self-sustaining combustion-oxidation of various finely ground metals. For the reduction step, established direct reduction iron (DRI) technology has been successfully used to convert solid iron ore into metallic iron without transitioning to the liquid phase.

Through thermodynamic calculations conducted using Aspen, ensuring precise process modelling and efficiency evaluation, this study examines the technical feasibility and preliminary design of an energy storage system that employs iron as a metallic energy carrier. Iron undergoes oxidation and serves as a fuel in high-temperature reactors operating above 1200 °C, thereby releasing its stored energy and forming iron oxide. When hydrogen is available, the iron oxide can be reduced back to metallic iron through the well-established Direct Reduced Iron (DRI) process or a comparable method at approximately 750 °C.

A round-trip thermal efficiency of 77.9 % has been calculated for the overall energy storage and utilization process. To further enhance global efficiency, key recommendations include hydrogen recirculation during the reduction process to ensure complete conversion and mitigating the impact of excess air in the oxidation stage.

1. Introduction

The transition to renewable energy is crucial for achieving net-zero CO_2 emissions and limiting global temperature rise to 1.5 °C above pre-industrial levels [1]. However, the integration of renewable sources presents challenges due to their intermittent nature, requiring efficient energy storage solutions to ensure a stable power supply, enhance grid reliability, and minimize infrastructure costs. Among the available storage options, renewable hydrogen produced via electrolysis has gained significant attention. Despite its versatility, its application for large-scale or long-term storage is limited due to its low volumetric energy density [2,3].

Metal fuels, such as iron, aluminium, magnesium, and silicon, have emerged as a promising alternative for energy storage [4,5].Their high energy density, long-term stability, and potential for cost-effective storage make them attractive for large-scale applications [6]. Unlike hydrogen, metal fuels can store energy in a compact form, making them suitable for space-constrained applications [7]. Energy is released through controlled oxidation, which can be harnessed as heat or electricity, providing a reliable and efficient storage solution [8]. Additionally, their ability to maintain performance over extended periods makes them a viable option for seasonal energy storage.

In the case of iron, an additional advantage lies in cost reduction and the extensive expertise in oxidation and reduction processes, which stems from the established practices of the iron and steel industry. In its metallic form, iron can be directly combusted with oxygen from the air to produce two primary stable oxides: magnetite (Fe_3O_4) and hematite (Fe_2O_3). These are exothermic reactions that occur rapidly at elevated temperatures, releasing heat as iron undergoes oxidation. The released thermal energy can be harnessed for use in thermal energy systems. The overall process is governed by the following global reactions [9]:

$$2\,Fe + 3/2\,O_2 \rightarrow Fe_2O_3 \quad \Delta H_r\,(298\ K) = -823.46\ kJ\ mol^{-1} \tag{1}$$

$$3\,Fe + 2\,O_2 \rightarrow Fe_3O_4 \quad \Delta H_r\,(298\ K) = -1117.31\ kJ\ mol^{-1} \tag{2}$$

According to the literature, the actual proportions of ferrite (Fe), wüstite (FeO), magnetite, and/or hematite found in the reaction products of iron-based combustors depend on multiple variables. Choisez et al [10] observed a complex microstructure consisting of wüstite, magnetite, and/or hematite after burning iron powder in pre-heated air.

☆ This article is part of a special issue entitled: 'INFUB 14' published in Thermal Science and Engineering Progress.

* Corresponding author.
E-mail address: luismi@unizar.es (L.M. Romeo).

https://doi.org/10.1016/j.tsep.2025.103721
Received 28 October 2024; Received in revised form 6 May 2025; Accepted 24 May 2025
Available online 26 May 2025

The ferrite content was estimated to be approximately 10 % based on SEM imaging. Traces of wüstite (FeO) were also detected, though the quantities were too small for quantitative analysis (less than 1 %). The remaining composition consisted of nearly equal proportions of hematite and ferrite.

A laboratory-scale cyclonic metal burner was employed in Eindhoven University to analyse gas temperature profiles, particle temperatures, exhaust gas compositions, and the resulting iron oxide morphologies [11]. The study revealed that iron powder ignited at temperatures above 823 K (550 °C) but the temperature has to be increased up to 1100 K (827 °C) with low oxygen concentration in the reactor. The same cyclonic metal combustor was also used to investigate the formation of nanoparticles and NO_x emissions during iron powder combustion under varying conditions of equivalence ratio and oxygen concentration [12]. The highest reference gas temperatures were observed when the input equivalence ratio—defined as the ratio of the mass of Fe to the mass of O_2 relative to stoichiometric conditions—was set to stoichiometry, based on the conversion of iron to magnetite, for each oxygen concentration. Similar trends were noted for varying proportions of Fe, FeO, Fe_2O_3, and Fe_3O_4, depending on the oxygen concentration in the flue gases and the input equivalence ratio. Higher oxygen concentrations (21 %) and lower equivalence ratios resulted in a greater proportion of Fe_2O_3 and Fe_3O_4, with each accounting for 40–50 % of the total composition. In contrast, lower oxygen concentrations (13.5 %) and higher equivalence ratios led to a higher proportion of unreacted Fe (up to 65 %) and greater levels of Fe_3O_4 compared to Fe_2O_3. It can be concluded that the stability of the burner and the composition of the residues was found to be highly dependent on the operating conditions, particularly oxygen concentration. For low values of oxygen, relevant amounts of unreacted ferrite were reported, as well as FeO.

Nearly complete oxidation was reported by Wiinikka et al. [13], who used a reactor with 21 % oxygen and a prolonged residence time of over one second, resulting in exceptionally high oxidation rates. The solid combustion products consisted of 96 % hematite (α- Fe_2O_3) spheres, with the remaining 4 % composed of maghemite (γ- Fe_2O_3). Thermodynamic calculations indicated that this product composition suggested near-complete combustion, with a conversion rate exceeding 98 %. So, it is evident that final oxidation composition is largely dependent on the design of the system (e.g., fuel and oxidizer distribution) and the operational conditions. High oxygen concentrations and reactor temperatures are needed to avoid the presence of Fe or FeO in the oxidation products. Different proportions of hematite and magnetite can be found in the solid oxides.

Regarding reduction, iron oxides (hematite/magnetite formed in the oxidation), can be regenerated back into metallic iron using hydrogen as reducing agent. The endothermic process reactions are [14]:

$$Fe_2O_3 + 3\ H_2 \rightarrow 2\ Fe + 3\ H_2O \quad \Delta Hr\ (298\ K) = +100.06\ kJ\ mol^{-1} \quad (3)$$

$$Fe_3O_4 + 4\ H_2 \rightarrow 3\ Fe + 4\ H_2O \quad \Delta Hr\ (298\ K) = +151.12\ kJ\ mol^{-1} \quad (4)$$

According to several reviews [15,16] and experimental works [17], hydrogen (H_2) has been demonstrated to be a more effective reducing agent than carbon monoxide (CO) for both thermodynamic and kinetic reasons, largely attributed to its superior diffusion properties. The initial reduction step, involving the conversion of Fe_2O_3 to Fe_3O_4 below 570 °C, occurs at a faster rate compared to the subsequent reduction of Fe_3O_4 to either $Fe_{1-y}O$ (wüstite) or Fe.

Temperature exerts a critical influence on these reactions. It is well-established that the reduction of hematite (Fe_2O_3) by hydrogen proceeds in two or three distinct stages, depending on whether the temperature is below or above 570 °C.

$$Fe_2O_3 \rightarrow Fe_3O_4 \rightarrow Fe\ (\text{below } 570\ °C) \quad (5)$$

$$Fe_2O_3 \rightarrow Fe_3O_4 \rightarrow FeO \rightarrow Fe\ (\text{above } 570\ °C) \quad (6)$$

The reduction of Fe_2O_3 by hydrogen within the temperature range of 220–680 °C has been deeply studied. Researches have focused on identifying the rate-controlling processes over the broadest and lowest possible temperature range. The findings indicated that the reduction followed the patterns outlined in Bell's Diagram [17].

Hessels et al. [18], examined the hydrogen reduction of iron oxide fines, produced by iron combustion, using thermogravimetric analysis (TGA) in the temperature range of 400–900 °C, with hydrogen partial pressures between 0.25 and 1.0 atm. Their experimental results revealed that the formation and morphology of pores in the particles—specifically pore size and quantity—are strongly influenced by the reduction temperature.

Similarly, Cerciello et al. [19] studied the reduction kinetics of iron ore with hydrogen and its subsequent re-oxidation with air using TGA over repeated reduction/oxidation cycles. They demonstrated that the choice between non-isothermal and isothermal kinetic analysis significantly impacts the kinetic rate parameters, largely due to the shift in the reduction pathway at a threshold temperature of 550–600 °C, where the reaction transitions from two stages to three. Additionally, they observed that the rate of oxidation decreases markedly after extensive reduction with hydrogen.

Addressing challenges related to specific oxidation and reduction processes, as well as other issues such as safety and cycling efficiency, is essential for advancing iron fuel technology to an industrial scale [20]. However, the significance of metal fuels in the evolving energy landscape cannot be overlooked. Ongoing research and development efforts are critical, as they assess the technical feasibility and provide key performance indicators necessary to realize the full potential of metal fuels as sustainable and environmentally friendly energy storage solutions.

Transitioning from a specific reactor to a system-level perspective, the design of high-temperature reactors, combined with an efficient heat network that optimizes high-temperature heat streams, is essential for achieving high round-trip efficiency. A well-engineered system that effectively integrates and utilizes the released energy is essential for optimizing performance. Current estimates suggest that the maximum electricity-to-electricity round-trip efficiency could reach approximately 40 %, factoring in electrolyser efficiency, through improvements in recycling processes and high- efficiency reactor design [4]. Even higher round-trip efficiencies could be attained when converting electricity or hydrogen directly to heat.

There remains a shortage of comprehensive feasibility studies on iron fuel technology. One of the most significant recent contributions [21] links process simulation with the kinetics of iron oxide reduction, proposing potential operational parameters. It may also be beneficial to review other high-temperature solid looping cycle applications to apply lessons learned in managing and designing high-temperature heat networks [22,23].

The technology, as an integrated system, has already been demonstrated at an industrial scale by TU Eindhoven in a brewery [24,25]. Since that demonstration, various industrial companies have made efforts to promote the development and commercialization of the concept, with innovations aimed at advancing its practical applications [26].

This study aims to assess the technical feasibility of utilizing iron as an energy carrier and to develop a preliminary design for an iron-based energy storage system. Thermodynamic calculations performed using Aspen enable accurate process modelling and facilitate the calculation of key performance indicators for the proposed technology.

2. Process description

The overall energy production and storage cycle can be divided in two temporally and spatially decoupled processes: oxidation (production, energy release) and reduction (energy storage) of the metal fuel. The process flow diagram is schematically illustrated in Fig. 1.

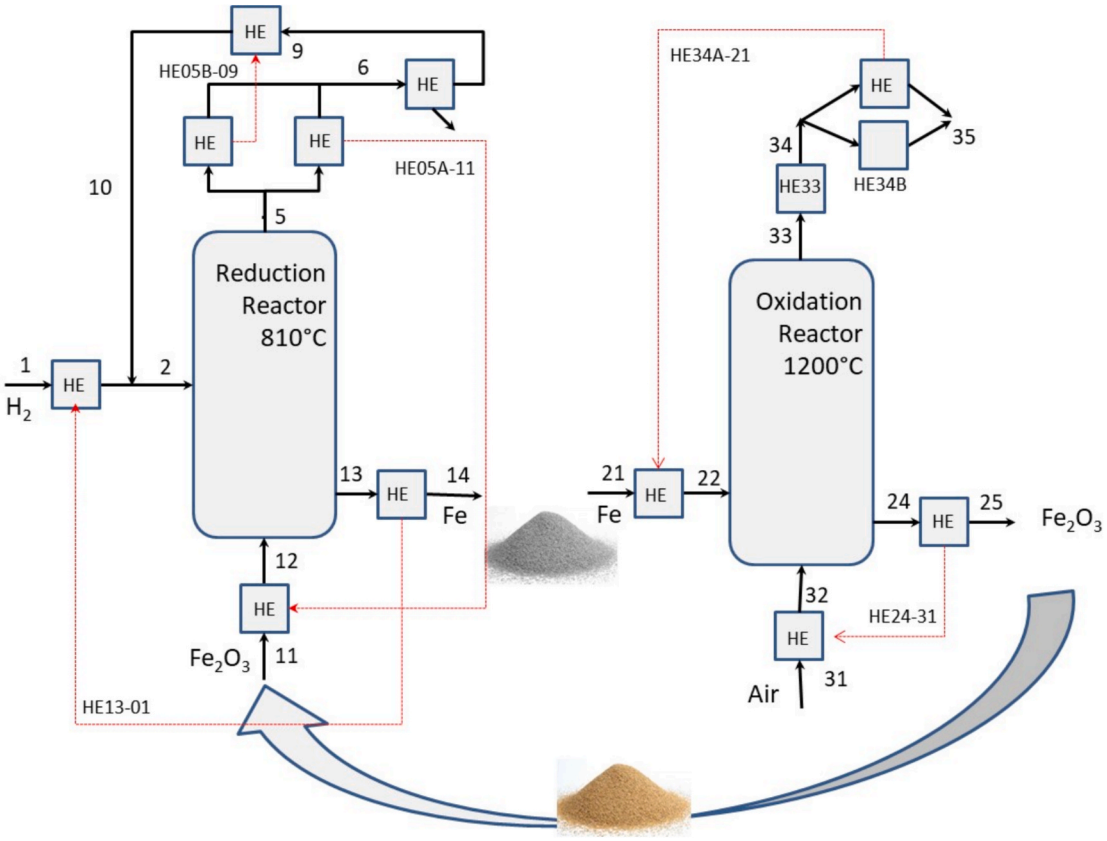

Fig. 1. Process layout. Hematite/Magnetite reduction reactor, iron oxidation reactor and heat exchangers (HE).

2.1. Oxidation

In its metallic form, iron can be directly combusted with oxygen from the air, generating two primary stable oxides: magnetite (Fe_3O_4) and hematite (Fe_2O_3). As established in the introduction through a review of the literature, the final oxidation products depend on several factors, such as system design and operational conditions [10,11,12,13]. While optimal conditions can minimize unreacted iron, both hematite and magnetite are typically present in the products. For the simulation reference case, based on experiments with ~70 μm iron particles under realistic conditions [27], a composition of 30 % hematite and 70 % magnetite has been selected. Both oxidation reactions are exothermic and occur rapidly at high temperatures, releasing heat that can be harnessed in thermal energy systems. The input equivalence ratio also plays a critical role in determining the extent of the reaction. An initial equivalence ratio (defined as the ratio of moles of oxygen in relation to the stoichiometric based in the inlet composition 30 % hematite and 70 % magnetite) of $\lambda_{O2} = 1.30$ has been chosen as a reference case.

A thermodynamic simulation of the oxidation process was conducted using Aspen Plus V12.1 software to analyse the influence of the oxygen equivalence ratio (λ_{O2}) through a sensitivity analysis. The inputs for the simulation consisted of preheated air and iron streams, with the oxidation reactor modelled as a RStoic reactor to account for the expected outputs and reactor temperatures. Key output variables included the energy released during combustion at a reactor temperature of 1200 °C, which could be harnessed for industrial applications, and the oxygen concentration at flue gas outlet, and the mass flow of solid oxides produced at 1200 °C.

Particularly, iron combustion does not produce CO_2 emissions. However, given the high combustion temperatures (above 1200 °C), existing techniques for reducing thermal NOx emissions could be employed if necessary. The products of the reaction, including flue gases and hematite, exit the reactor at elevated temperatures, allowing for the recovery of sensible heat. This heat can be used to preheat iron and air, while additional excess heat from the reactor and other heat exchangers can be repurposed for industrial processes.

Fig. 2 illustrates the results of varying the proportion of hematite (with respect to magnetite) in the output iron oxides. An increased formation of hematite corresponds to a greater energy release in the oxidation reactor (Q_{react}), increasing from 4908 to 5409 kW/kg_{fuel} (0.204 to 0.185 kg_{fuel}/MW), along with a higher oxygen consumption, which significantly reduces the O_2 content in the flue gases. The variable Q_{total} represents the total heat available, including the heat that can be utilized within the reactor, as well as the sensible heat of both the gases and the iron oxides. To maintain a conservative approach in the energy

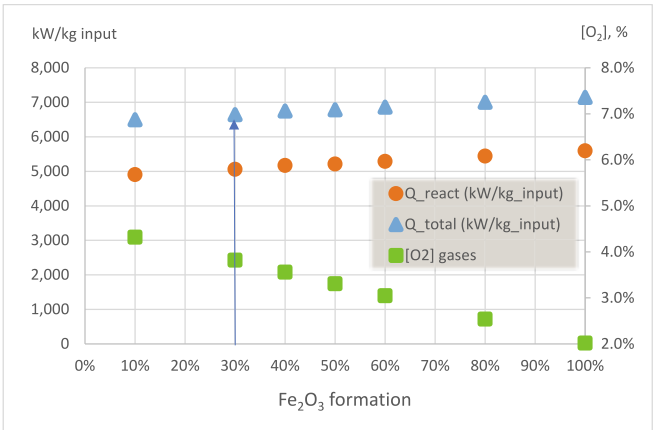

Fig. 2. Heat released in the reactor and in the process (kW/kg Fe), O_2 concentration %vol. in flue gases as a function of Fe_2O_3 formation in the oxidation reactor.

analysis, the initial assumption of complete iron reaction to 30 % hematite and 70 % magnetite, as obtained in preliminary oxidation experiments in suspended burner at realistic conditions [27], has been retained for subsequent calculations.

2.2. Reduction

Iron oxides, such as hematite (Fe_2O_3) and magnetite (Fe_3O_4), can be regenerated into metallic iron by using hydrogen as a reducing agent. When hydrogen is produced from renewable energy sources, this charge–discharge cycling process offers a zero-carbon energy storage solution. The intermittent nature of regeneration does not pose significant operational challenges, though maintaining a small buffer of H_2 would enhance the management and efficiency of the reduction process. The key reactions involved in the reduction process are as follows:

$$Fe_2O_3 + (3 + x)\ H_2 \rightarrow 2\ Fe + 3\ H_2O + x\ H_2 \quad (7)$$

$$Fe_3O_4 + (4 + y)\ H_2 \rightarrow 3\ Fe + 4\ H_2O + y\ H_2 \quad (8)$$

These reduction reactions are endothermic. To model the process, a reduction simulation was developed using an RGibbs reactor provided by Aspen Plus V12.1 software. This unit calculates the thermodynamic equilibrium of the system by minimizing the total Gibbs free energy of all the components present in the reactor. The selection of Gibbs free energy minimization influences chemical equilibrium and increases hydrogen requirements but, as the excess hydrogen is recovered and recycled, it enables highly favourable gas oxidation degree (GoD) conditions for the complete reduction of iron oxides without increasing the total hydrogen demand or energy requirements.

In previous studies, it was suggested that burning a small amount of the hydrogen injected for the reduction could supply the necessary energy to maintain the reactor around 800 °C [27]. However, the simulation results aligned with findings from several literature studies, indicating that the minimization of Gibbs free energy leads to the formation of FeO (wüstite), a common outcome in the presence of water vapour. Water vapour in the reducing gas significantly affects the reduction process in two ways: first, it reduces the thermodynamic driving force for reduction, and second, it adsorbs onto the reaction surface, blocking available sites and preventing hydrogen from effectively reducing the iron oxides [16]. This dual effect is temperature-dependent. At lower temperatures, water vapour adsorption is more prominent, hindering the reduction process, while at higher temperatures, the impact of adsorption decreases, allowing for more efficient reduction. To mitigate these effects, in the present calculations the stream of hydrogen and solid oxides have been preheated to the maximum temperature achievable with other heat streams from the process and no hydrogen is burned in the reduction reactor. Calculations show the external heat required in reduction reactor to maintain the temperature and provide the reduction reaction energy. This approach aims to minimize the influence of water vapour and improve overall reduction efficiency.

In order to determine the required hydrogen mass flow for complete reduction of the solid oxides (composed of 30 % hematite and 70 % magnetite as produced in the oxidation reactor), some preliminary calculations were conducted. In this analysis, the H_2 mass flow rate per kilogram of solid oxides at the reactor inlet was varied. Fig. 3 presents the results for a reduction temperature of 830 °C. It may be inferred that there is a minimum H_2 mass flow required to achieve complete conversion of the solid oxides. At 830 °C, when the H_2 mass flow is increased from 0.15 to 0.20 kg/s, the hydrogen content in the flue gases remains constant, but the FeO content in the solid particles decreases to zero. This reduction in FeO corresponds to an increase in the metallic iron (Fe) content, indicating full conversion of the solid oxides. Beyond this point, any excess H_2 is detected in the gas phase, as further increases in hydrogen flow do not contribute to additional oxide reduction.

Fig. 4 extends this calculation to illustrate the minimum hydrogen mass flow required for complete conversion of solid oxides as a function of temperature. The results show that the required H_2 steadily decreases as the reduction reactor temperature increases. Additionally, the total heat required for the entire reduction process, or specifically for the reduction reactor, reaches a minimum around 810 °C. Beyond this temperature, the heat requirement begins to rise, though the increase is relatively modest and does not significantly impact the overall energy demand of the process.

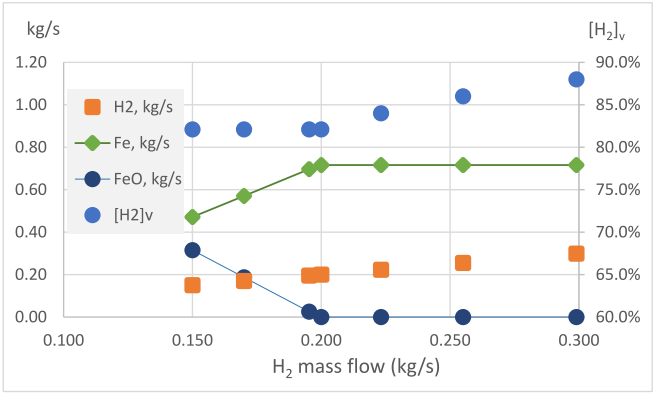

Fig. 3. H_2 concentration in flue gases, FeO and Fe contents in solid particles (per kg of solid oxides) after reduction with different H_2 inlet mass flows.

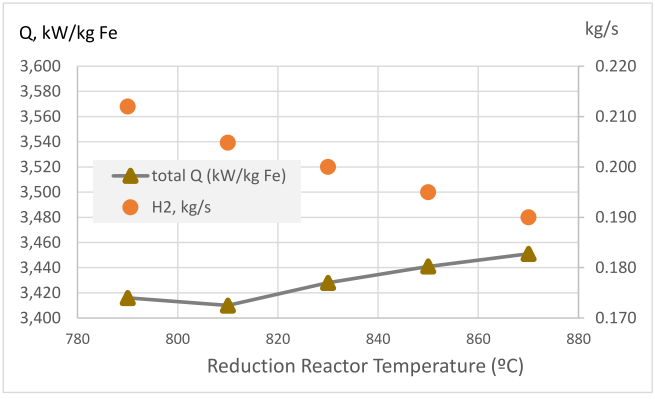

Fig. 4. Total heat demanded in the reduction process and minimum H_2 mass flow to achieve complete solid oxides conversion (1 kg) as a function of temperature.

3. Process model setup

The entire process, which comprises two independent sub-processes—oxidation and reduction—was simulated using Aspen Plus V12.1 software. The corresponding process schemes are presented in Figs. 5 and 6. This simulation aimed to conduct a technical analysis and generate key performance indicators (KPIs) for the system, as summarized in Table 4. The most relevant KPIs include energy efficiency in the reduction and oxidation stages, various mass flow ratios of H_2 and O_2 required per kilogram of iron or iron oxides, and the overall round-trip efficiency of the entire process. The following key assumptions were made:

- The oxidation and reduction processes are temporally and spatially decoupled. To facilitate the calculations, a reference input mass flow rate of 1 kg/s of iron in the oxidation reactor and an output mass flow rate of 1 kg/s of solid oxides in the reduction reactor has been adopted.

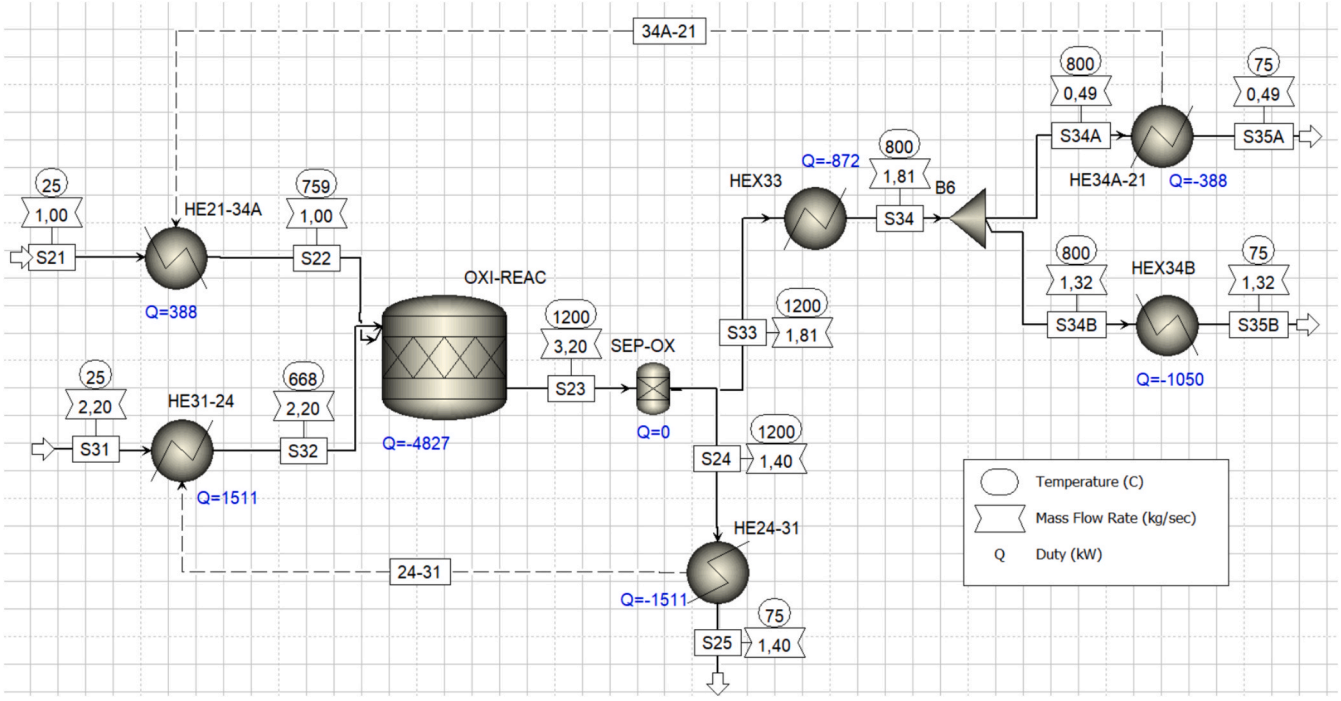

Fig. 5. Aspen Plus schematic of the oxidation sub-process.

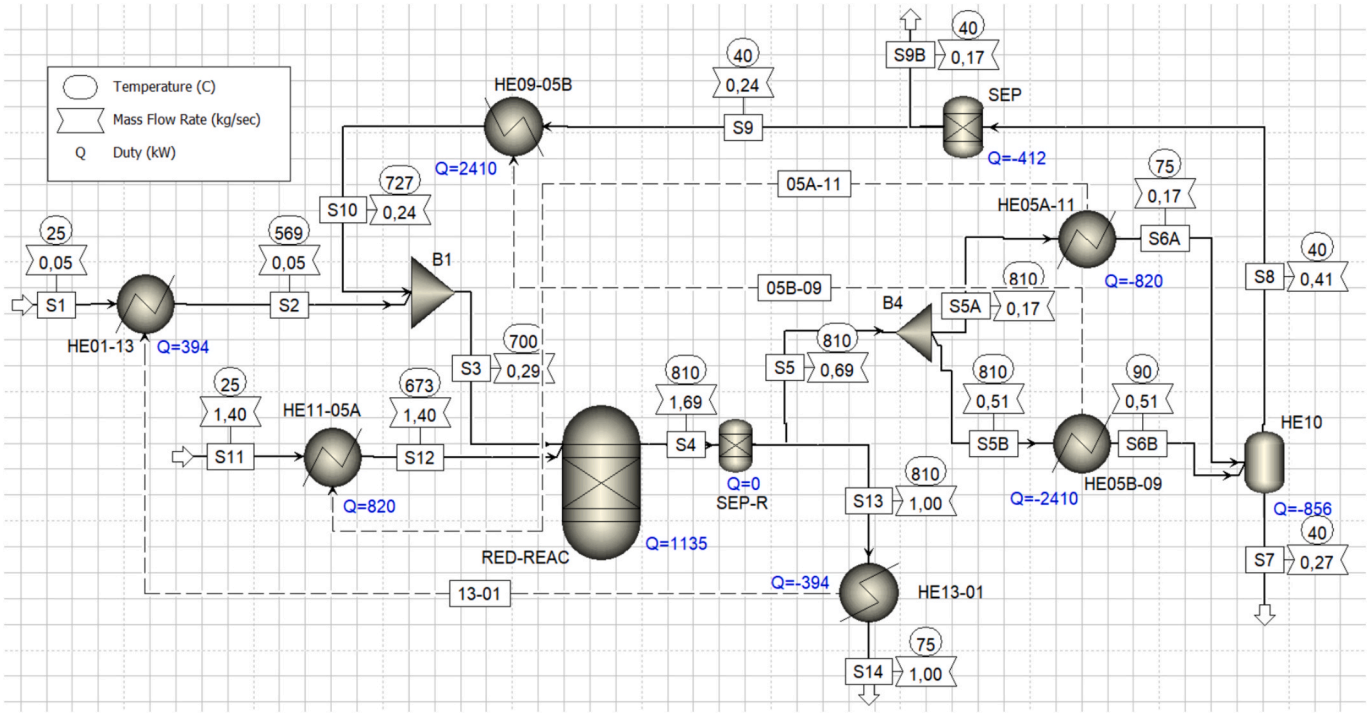

Fig. 6. Aspen Plus schematic of the reduction sub-process.

- In the oxidation reactor, the reactants—iron and air—are introduced at an ambient temperature of 25 °C. This assumption supports the feasibility of long-term energy storage, as iron possesses favourable storage properties at ambient temperature, contributing to the reduction of storage-related costs.
- Iron fully reacts into 30 % hematite and 70 % magnetite and an excess air ratio of $\lambda_{O2} = 30$ % above the stoichiometric requirement is maintained in the oxidation reactor.
- The operating temperature of the oxidation reactor has been set at 1200 °C after the observations of Wiinika [13] that burnt sponge iron in an externally heated entrained flow reactor at 1200 °C, finding nearly full oxidation of the fuel to Fe_2O_3. Although particle temperature ranges 1200 to 2200 K according previous works (Jimenez et al. [28]), the average gas temperature profile indicates lower reactor temperatures and 1200 °C is a good estimation of our experimental findings. Assuming higher reactor temperatures, the

heat recovered within the reactor decreases, while the sensible heat of solids and gases increases proportionally. Consequently, although reactor temperature may be a degree of freedom in the model, it does not impact key performance indicators but rather influences energy distribution between the reactor and subsequent heat exchangers.

- The oxidized product leaving the reactor is a solid oxide mixture containing 30 % Fe_2O_3 and 70 % Fe_3O_4. This solid oxide product exits the oxidation reactor at 1200 °C, and a high-temperature heat exchanger is used to recover heat and then preheat the incoming air (HE24-31).
- The flue gas exits the oxidation reactor at 1200 °C, below the melting points of iron (1530 °C) and hematite (1560 °C) [26], where and a high-temperature heat exchanger (HEx33) and a medium-temperature heat exchanger (HEx34B) recover heat to be used in industrial processes.
- The operating temperature of the reduction reactor is set at 810 °C, in order to maximize the efficiency. According to the preliminary calculations shown in Fig. 4, the lowest energy requirements for the reduction stage occur at a reactor temperature of 810 °C. When the total hydrogen flow into the system is reduced, the overall energy demand in the reduction stage increases slightly; therefore, a reactor temperature of 810 °C has been assumed.
- A high gas oxidation degree (GoD) is selected to ensure the complete reduction of iron oxides. Excess hydrogen is recovered and recycled, minimizing net H_2 requirements to only the amount necessary for full iron oxide reduction. This approach also minimizes the impact of reactor modelling choices on the overall process.
- The minimum temperature difference across heat exchangers is 50 °C, which is appropriate for, both, solid–gas and gas–gas heat exchangers.
- The minimum temperatures of the gas and solid particles after cooling are set at 75 °C to ensure a temperature difference of 50 °C relative to the ambient temperature. The sensible heat lost in solids (iron and iron compounds) and gases (oxygen-depleted air, hydrogen with water vapour) as they cool from 75 °C to ambient temperature reduces the efficiency of both the reduction and oxidation stages.

4. Results and process analysis

Table 1 summarizes the key stream data for the design operating point. As previously mentioned, for the oxidation reactor a reference mass flow of 1 kg/s of iron (stream 21) at ambient temperature 25 °C is used. Solid-gas heat exchanger HE34A-21 supplies the energy required to increase the temperature of the iron from 25 °C to 759 °C (as shown in Table 2) while reduces the oxygen-depleted air temperature from 800 to 75 °C. The air entering the oxidation reactor is preheated to 668 °C in another solid–gas heat exchanger HE24-31 using the solid oxides formed during combustion. Table 2 presents the energy exchanged and the temperatures of all streams involved in the heat exchanger. There are two additional heat exchangers, HEX33 and HEX34B, that facilitate energy transfer to an industrial process, as outlined in Table 3. These operate at two temperature levels: a high temperature range (1200 °C to 800 °C) and a medium–low temperature range (800 °C to 75 °C). Furthermore, since the oxidation reaction is exothermic, it releases additional heat in the reactor at 1200 °C, amounting to 4827 kW.

The reduction sub-process is more complex due to the endothermic nature of the reduction reaction, requiring both the hydrogen and solid oxide streams to be preheated before entering the reactor. The solid oxides (stream 11) are preheated using part of the flue gases (stream 5A, HE05A-11) exiting the reactor. In this process, the gas stream cools from 810 °C to 75 °C (820 kW), transferring heat to the solid oxides, which are heated from 25 °C to 673 °C in a gas–solid heat exchanger, maintaining the proposed minimum temperature difference of 50 °C. The remaining gases (stream 5B) are utilized to preheat the hydrogen stream in HE05B-09 (gas–gas heat exchanger) after the complete water separation and before the mix with the net input hydrogen to the process (stream 2). The cooling of the residual flue gases (H_2 + H_2O) facilitates the separation and condensation of water vapour from hydrogen. So, a heat

Table 2
Heat exchangers operational temperatures and energy transferred.

HE13-01	Hot (g), °C	Cold (g), °C	HE05A-11	Hot (g), °C	Cold (g), °C
Q 394 kW	T_{in} = 810.0 T_{out} = 75.0	T_{out} = 568.5 T_{in} = 25.0	Q 820 kW	T_{in} = 810.0 T_{out} = 75.0	T_{out} = 673.3 T_{in} = 25.0
HE05B-09		**Hot (g), °C**			**Cold (g), °C**
Q 2410 kW		T_{in}= 810.0 T_{out}= 90.0			T_{out}= 726.8 T_{in}= 40.0
HE34A-21	**Hot (g), °C**	**Cold (g), °C**	**HE24-31**	**Hot (g), °C**	**Cold (g), °C**
Q 388 kW	T_{in}= 800.0 T_{out}= 75.0	T_{out}= 759.0 T_{in}= 25.0	Q 1511 kW	T_{in}= 1200.0 T_{out}= 75.0	T_{out}= 668.3 T_{in}= 25.0

Table 1
Process conditions of the reduction–oxidation processes.

Stream	m (kg/s)	T (°C)		Stream	m (kg/s)	T (°C)	
S1	0.0499	25.0	$[H_2]$ = 100 %	**S21**	1.0000	100.0	$[N_2]$ = 79.0 % $[O_2]$ = 21.0 %
S2	0.0499	568.2		**S22**	1.0000	759.0	
S3	0.2900	699.8		**S23**	3.2020	1200.0	
S4	1.6863	810.0		**S24**	1.3963	1200.0	$[Fe_2O_3]_w$ = 30 % $[Fe_3O_4]_w$ = 70 %
S5	0.6860	810.0	$[H_2]$ = 82.8 % $[H_2O]$ = 17.2 %	**S25**	1.3963	75.0	
S5A	0.1715	810.0					
S5B	0.5145	810.0		**S31**	2.2020	25.0	
S6A	0.1715	75.0		**S32**	2.2020	668.3	
S6B	0.5145	90.0		**S33**	1.8057	1200.0	$[N_2]$ = 94.30 % $[O_2]$ = 5.70 %
S7	0.2748	40.0	$[H_2O]$ = 100 %	**S34**	1.8057	800.0	
S8	0.4112	40.0	$[H_2]$ = 100 %	**S34A**	0.4875	800.0	
S9	0.2400	40.0		**S34B**	1.3181	800.0	
S10	0.2400	726.8		**S35A**	0.4875	75.0	
S11	1.3963	25.0		**S35B**	1. 3181	75.0	
S12	1.3963	673.3					
S13	1.0000	810.0	100 % Fe				
S14	1.0000	75.0	100 % Fe				

Table 3
Available energy in heat exchangers not used internally in the process.

HE	HE3334	HE3435B	Ox reactor
Q	872 kW	1050 kW	4827 kW

exchanger reduces the temperature of the stream to just above its saturation point (HE10), and a final heat exchanger cools the stream, condensing water and drying the hydrogen stream, which is then recirculated. This cooling step is crucial for ensuring the efficient reuse of hydrogen in the system and maintaining the overall energy efficiency of the process. The hydrogen required for the reduction process is pre-heated using the solid iron exiting the reduction reactor. This takes place in a gas–solid heat exchanger (HE 13–01, 394 kW), raising the hydrogen temperature to 673 °C, with a final inlet temperature at the reactor of 700 °C.

Table 4 summarizes the key performance indicators (KPIs) for the overall process. Based on the assumption that the solid oxides contain 30 % hematite (Fe_2O_3) and 70 % magnetite (Fe_3O_4), the stoichiometric hydrogen-to-iron (H_2-Fe) ratio is calculated to be 1.37.

As previously discussed, the hydrogen required for the reduction has been determined as the minimum amount necessary to avoid the formation of FeO in the final iron product. This is calculated through the minimization of Gibbs free energy, resulting in an H_2-Fe ratio of 8.03 at 810 °C, which corresponds to 5.81 times the stoichiometric requirement. This ratio is relatively high compared to values reported in the literature. For instance, a ratio of 3 was proposed for reduction at 800 °C [21]. Neumann et al [29] have determined the hydrogen equivalence ratio required for the complete conversion to iron as a function of reaction temperature, assuming a co-current flow reactor with varying GOD at the reactor inlet. Their analysis indicates that for a GOD of zero and 800 °C, a ratio of 3.2 is necessary. However, they also conclude that a surplus of hydrogen is required in practical applications due to constraints imposed by reaction kinetics and transport phenomena, which influence the overall conversion process. But in this case, as the excess hydrogen is recovered and recycled, it does not increase the total hydrogen demand but enables highly favourable gas oxidation degree (GoD) conditions for the complete reduction of iron oxides.

For the oxidation process, the input oxygen-to-iron (O_2/Fe) ratio is set at 1.3 times the stoichiometric requirement (lean conditions) to achieve a conversion consisting of 30 % hematite and 70 % magnetite. This ratio is not expected to significantly affect the efficiency of the oxidation stage, as the energy content in the flue gases is effectively recovered. With a minimum temperature difference of 50 °C, the oxygen-depleted gases can be cooled to 75 °C, thereby minimizing energy losses in this stage.

With the specified input variables, the energy efficiency of the reduction process is calculated to be 85.2 %. This efficiency is defined as the ratio between the heating value of iron (7379 kJ/kg [9]) minus the heating value of iron oxides at input, and the total energy input for the reduction process, which includes both the High Heating Value (HHV) of hydrogen (HHV[H_2]) and the energy required in the reduction reactor (Q_{red}). Comparable efficiency values have been reported in the literature. For instance, an efficiency of 91 % was achieved for a hydrogen-to-iron ratio (λ_{red}) of 3 at 800 °C [21], assuming optimal heat recovery. In contrast, a more recent and comprehensive study [29], calculated a lower reduction efficiency of 79.5 %, which was further decreased when accounting for peripheral energy requirements specific to the reduction process. These discrepancies may arise from the fact that, in the present study, all residual energy from the solid iron and gas streams is fully recovered to preheat both the hydrogen and the solid oxides, thereby enhancing the overall efficiency of the reduction process. Nevertheless, the inclusion of auxiliary components such as fans, blowers, mills, and fuel handling systems will be necessary, which will consequently reduce the net process efficiency.

Table 4
Key performance indicators (KPI) of the whole process.

KPI	Formula	Value
$\lvert H_2/oxides\rvert_{mol}$	$n[S3]/n[S12]$	21.02
$\lvert H_2/Fe\rvert_{mol}$	$n[S3]/n[S13]$	8.03
$\lvert H_2/Fe\rvert_{molsto}$	$n[S3]_{est}/n[S13]$	1.37
λ_{red}, H_2/Fe reduction ratio	$n[S3]/n[S3]_{est}$	5.81
$\lvert O_2/Fe\rvert_{mol}$	$(n[31]*0.21)/n[S21]$	0.895
$\lvert O_2/Fe\rvert_{molsto}$	$(n[31]_{est}*0.21)/n[S21]$	0.685
λ_{oxi}, O_2/Fe oxidation ratio	$n[S3]/n[S3]_{est}$	1.30

KPI	Formula	Value
Energy Efficiency reduction	$\eta_{red} = (HHV[Fe] - HHV[Fe_xO_y])/(HHV[H_2] + Q_{red})$	85.2%
Energy Efficiency oxidation	$\eta_{oxy} = (Q_{oxi} + \sum Q_{HEx})/HHV[Fe]$	91.5%
Round trip efficiency	$\eta = \eta_{oxy} * \eta_{red}$	77.9%

A similar energy efficiency is achieved in the oxidation process, calculated at 91.4 %. This efficiency is the ratio between the heat recovered from the high-temperature oxidation reactor (operating at 1200 °C), which includes the heat released during oxidation, and the heat recovered through two heat exchangers that can be used as industrial heat stream, compared to the energy content in the metallic iron. The primary energy losses are attributed to the oxygen-depleted air streams, which are vented at 75 °C, and a small amount of residual energy that is lost when the solid oxides at 75 °C are stored for the reduction process at ambient temperature.

The obtained efficiency value is lower than those reported in previous studies [29], such as boiler efficiencies—comparable to the oxidation efficiency in this work—which are typically around 98.0 %. This discrepancy arises primarily from differences in the definition of efficiency. In this study, the higher heating value of iron is used as a reference, while the combustion process is assumed to result in 30 % hematite and 70 % magnetite, rather than complete oxidation. This partial oxidation accounts for a loss in efficiency of approximately five percentage points and represents the primary difference. Additional losses stem from the sensible heat of particles and flue gases.

Overall, the round-trip energy efficiency of the process—taking hydrogen as the input and heat as the output—is 77.9 %. While this is a relatively high efficiency, it is important to consider the efficiencies of hydrogen production and heat utilization, which can significantly reduce this value. These losses, however, are not directly related to the process under study but rather depend on the specific technologies. For instance, assuming an electrolyser electrical system efficiency of 74.1 % (target for 2050 [30]), a supercritical power generation cycle of 45 %, and a heat utilization efficiency of 95 % when directly applied in an industrial process, the overall power generation efficiency using iron-based energy storage without CO_2 emissions could exceed 26.0 This corresponds to an efficiency penalty of 19 percentage points, which is seven-eight points higher than that associated with commercial post-combustion [31] or oxyfuel [32] CO_2 capture technologies. However, in this case, energy storage is also incorporated. When the generated heat is utilized in industrial processes, the overall efficiency increases to 54.9 %.

Although the process simulation developed in Aspen Plus V12.1 offers a detailed and coherent framework for evaluating the iron-based energy storage system, several critical uncertainties must be acknowledged when extrapolating these results to a practical implementation. The model is based on key assumptions such as spatial and temporal decoupling of the oxidation and reduction processes, controlled reactor temperatures (1200 °C for oxidation and 810 °C for reduction), and a fixed mass flow of 1 kg/s of iron. In the reduction stage, the design assumes an entrained flow reactor operating at 810 °C with high gas–solid contact efficiency, a gas oxidation degree (GoD) sufficient to ensure full reduction, and hydrogen recycling to minimize consumption. The overall H_2-to-Fe mass flow ratio is derived from stoichiometric needs

and optimized for energy efficiency, yielding a value of approximately 0.12 kg H_2 per kg of Fe_2O_3 reduced, depending on the oxide mixture and recycling efficiency.

However, despite this level of detail, several uncertainties remain. First, the long-term cyclic stability of the iron particles is not yet experimentally validated at large scale. While the simulation assumes consistent particle reactivity and morphology, real-world conditions may lead to sintering, fragmentation, or passivation effects over multiple cycles, affecting system efficiency and material handling. Second, although the reactor temperatures are carefully selected based on thermodynamic and kinetic considerations, maintaining these precise thermal conditions in practice will require advanced control strategies, insulation, and robust heat integration, especially considering possible heat exchanger degradation or fluctuating load conditions. Third, auxiliary energy demands—such as for gas compression, solid transport, and thermal losses in the reactor walls—are partially considered but could be underestimated, reducing the net round-trip efficiency. Finally, the simulation assumes ideal reactor operation with homogeneous flow and perfect heat and mass transfer, but the real performance of the reduction reactor, including gas–solid distribution, residence time uniformity, and catalyst-free operation, may deviate from model predictions. Overall, while the process design and KPI projections are promising, these uncertainties emphasize the need for continued experimental validation and pilot-scale testing, particularly to confirm material durability, heat recovery effectiveness, and reduction reactor performance under cyclic and transient conditions.

4.1. H_2 mass flow influence on reduction process

The simulation conditions provide limited potential for further improvements in round-trip efficiencies. In the reduction process, the minimum hydrogen flow required for complete reduction has been carefully selected to prevent the formation of FeO, based on the RGibbs function in ASPEN. Although the hydrogen-to-iron (H_2/Fe) ratio exceeds the values reported elsewhere [21], this higher ratio is essential to promote favourable gas oxidation degree (GoD) conditions and ensure the complete reduction of iron oxides. The recirculation of unutilized hydrogen enables a significantly higher GoD and facilitates complete conversion at lower temperatures.

Lower hydrogen recirculation rates have been shown to allow FeO formation, which decreases the amount of iron produced. This not only compromises the reduction process but also diminishes the efficiency of the oxidation process, as it reduces the amount of iron available for storage and subsequent oxidation, leading to a lower overall system efficiency.

Although the H_2/Fe ratio is already elevated, simulations were conducted to examine the effects of further increasing hydrogen injection. The results indicate that higher H_2 ratios do not alter the solid output, and any excess hydrogen must be cooled and recirculated back to the reactor. For example, increasing the hydrogen mass flow by 10 % raises the H_2/Fe ratio to 6.45 (over stoichiometric) and slightly decreases the overall energy efficiency of the reduction process to 85.05 %.

With this increased ratio, a reduction in the reactor temperature becomes possible while still achieving complete reduction. According to the simulations, a reactor temperature of 770 °C can be maintained with an H_2/Fe ratio of 6.45. However, the effect on the overall energy efficiency is negligible, as the heat recovered from the streams exiting the reactor is also reduced. This, in turn, lowers the inlet stream temperatures, balancing out the potential energy gains from the reduced reactor temperature. Thus, the benefits of higher hydrogen injection are minimal in terms of improving energy efficiency. Therefore, the primary recommendation is to keep the hydrogen mass flow at the lowest possible level to ensure complete reduction conversion.

4.2. Oxygen excess influence on oxidation process

Table 5 presents the results of the influence of excess air on the oxidation process, again assuming oxidation to a mix of 30 % hematite and 70 % magnetite. Increasing the air mass flow reduces the amount of heat recovered at high temperatures from the oxidation reactor while increasing the heat recovered in the heat exchangers at lower temperatures. This second effect partially compensates for the heat loss in the reactor, and as a result, the overall effect on energy efficiency is minimal. For instance, a 10 % increase in air mass flow—from 2.20 to 2.37 kg/s per kg/s of iron (corresponding to an excess air factor from 1.30 to 1.40)—leads to a modest decrease in the energy efficiency of the process by around 0.30 percentage points.

Table 5 also details the distribution of energy between the reactor and heat exchangers. If heat is only recovered from the reactor (first quantity in Table 5), the impact of excess air is more pronounced. For example, the efficiency drops significantly from 69.2 % with an excess air factor of 1.15, to 62.9 % when the excess air is increased to 1.40. Additionally, the oxygen content in the flue gases increases from 3.3 % to 7.0 % as the excess air rises. Consequently, the negative impact of excess air is not as significant as that of increased hydrogen mass flow. In any case, further experimentation on the oxidation reaction is necessary to deepen our understanding, given its high sensitivity to multiple factors such as reactor design, solid particle diameters, oxygen content and distribution, temperature, and other operational parameters. These variables can significantly affect the oxidation process and its overall efficiency, underscoring the need for more detailed investigations.

5. Conclusions

The transition to renewable energy requires the development of energy storage systems that are efficient, feasible, reliable, zero-carbon, and environmentally sustainable. Recyclable metals, such as iron, are among the most attractive chemical energy carriers due to their energy density and recyclability. In this study, the technical feasibility and preliminary design of an energy storage system utilizing iron as the energy carrier have been investigated.

In this concept, iron is oxidized in high-temperature reactors or boilers, releasing its stored energy and producing iron oxide as a by-product. The iron oxide can then be regenerated back into iron through a reduction process using renewable hydrogen. This cycle offers a potentially sustainable method of storing and utilizing energy, aligning with the goals of carbon neutrality and environmental sustainability in energy systems.

A simulation of the overall energy cycle has been conducted using Aspen 12.1. For the reduction process, an energy efficiency of 85.2 % was achieved, using a mixture of 30 % hematite and 70 % magnetite as the solid iron oxides. A critical aspect of this process is maintaining the minimum hydrogen-to-iron (H_2/Fe) ratio required to achieve complete reduction of the iron oxides, thereby avoiding the formation of FeO. A high over-stoichiometric H_2/Fe ratio of 5.81 has been selected to achieve favourable GoD conditions and ensure the complete reduction of iron oxides. The recirculation of unutilized hydrogen supports this higher GoD and facilitates full conversion at lower temperatures. Increasing the H_2/Fe ratio beyond this point does not improve the reaction performance or energy efficiency and would lead to higher costs due to the need for larger installations to accommodate the increased

Table 5
Influence of air excess in the oxidation sub-process.

Air mass flow rate (kg/s)	Excess air ratio	Heat available in reactor and HExs (kW)	[O_2] in flue gases, %
2.37	1.40	4642/953/ 1146 = 6741	7.0
2.20	**1.30**	**4827/872/1050 = 6749**	**5.7**
1.95	1.15	5104/752/905 = 6761	3.3

hydrogen volume. Thus, this ratio strikes a balance between process efficiency and cost-effectiveness, ensuring complete reduction without unnecessary resource expenditure.

A conservative assumption of 30 % hematite and 70 % magnetite composition at the outlet was used in the oxidation process simulation. Under conditions of 1.30 excess air, a reactor temperature of 1200 °C, and heat recovery down to 75 °C, the process achieved an efficiency of 91.4 %. Since the oxidation reaction is highly sensitive to various operational parameters—such as reactor design, particle size of the solids, oxygen content and distribution, temperature, and other factors— the impact of excess air was also investigated, demonstrating that maintaining low levels of excess air is crucial for achieving high energy efficiency. Excess air beyond the optimal level leads to reduced heat recovery and efficiency losses.

The round-trip efficiency of the overall energy storage and utilization process, from hydrogen to heat, was calculated to be a maximum of 77.9 %, excluding auxiliary components. This assumes no limitations in storage capacity or time, highlighting the potential of this system in large-scale energy applications. This value falls between the round-trip efficiencies of a hydrogen storage system combined with a combustor for heat generation, with reported literature values of 87 % for compressed hydrogen at 800 bar and 71 % for liquefied hydrogen storage [33]. However, further experimental research is necessary to confirm the operational feasibility of reduction with lower hydrogen-to-iron ratios and to develop a deeper understanding of the variables that influence iron oxidation.

Declaration of Generative AI and AI-assisted technologies in the writing process

During the preparation of this work, the authors used ChatGPT in order to improve readability and language. After using this tool, the authors reviewed and edited the content as needed and take full responsibility for the content of the publication.

CRediT authorship contribution statement

Luis M. Romeo: Writing – original draft, Visualization, Validation, Supervision, Methodology, Investigation, Formal analysis, Conceptualization. **Javier Saez-Guinoa:** Writing – review & editing, Supervision, Investigation, Formal analysis. **Santiago Jiménez:** Writing – original draft, Visualization, Validation, Methodology, Conceptualization. **Carmen Mayoral:** Writing – original draft, Validation, Project administration, Investigation, Funding acquisition, Formal analysis, Conceptualization.

Declaration of competing interest

The authors declare that they have no known competing financial interests or personal relationships that could have appeared to influence the work reported in this paper.

Acknowledgements

The work presented in this paper has been funded by the R&D Spanish National Program and the European Regional Development Funds (European Commission), under project NewIronAge, PID2022-141372OB-I00 and it is also supported by the Government of Aragon (Energía y CO2. Research Group DGA T46_17R).

Data availability

Data will be made available on request.

References

[1] United Nations. The Paris Agreement | UNFCCC 2015. https://unfccc.int/process-and-meetings/the-paris-agreement (accessed November 6, 2023).
[2] W. He, M. King, X. Luo, M. Dooner, D. Li, J. Wang, Technologies and economics of electric energy storages in power systems: review and perspective, Adv. Appl. Energy 4 (2021) 100060, https://doi.org/10.1016/J.ADAPEN.2021.100060.
[3] J. Andersson, S. Grönkvist, Large-scale storage of hydrogen, Int. J. Hydrogen Energy 44 (2019) 11901–11919, https://doi.org/10.1016/J.IJHYDENE.2019.03.063.
[4] J.M. Bergthorson, Recyclable metal fuels for clean and compact zero-carbon power, Prog. Energy Combust. Sci. 68 (2018) 169–196, https://doi.org/10.1016/J.PECS.2018.05.001.
[5] J.M. Bergthorson, S. Goroshin, M.J. Soo, P. Julien, J. Palecka, D.L. Frost, et al., Direct combustion of recyclable metal fuels for zero-carbon heat and power, Appl. Energy 160 (2015) 368–382, https://doi.org/10.1016/J.APENERGY.2015.09.037.
[6] P. Julien, J.M. Bergthorson, Enabling the metal fuel economy: green recycling of metal fuels, Sustain. Energy Fuels 1 (2017) 615–625, https://doi.org/10.1039/C7SE00004A.
[7] L. Dirven, N.G. Deen, M. Golombok, Dense energy carrier assessment of four combustible metal powders, Sustain. Energy Technol. Assessments 30 (2018) 52–58, https://doi.org/10.1016/J.SETA.2018.09.003.
[8] P. Debiagi, R.C. Rocha, A. Scholtissek, J. Janicka, C. Hasse, Iron as a sustainable chemical carrier of renewable energy: analysis of opportunities and challenges for retrofitting coal-fired power plants, Renew. Sustain. Energy Rev. 165 (2022) 112579, https://doi.org/10.1016/J.RSER.2022.112579.
[9] S.H. Fischer, M.C. Grubelich, Theoretical Energy Release Of Thermites, Intermetallics, and Combustible Metals, 1998, doi: 10.2172/658208.
[10] L. Choisez, N.E. van Rooij, C.J.M. Hessels, A.K. da Silva, I.R.S. Filho, Y. Ma, et al., Phase transformations and microstructure evolution during combustion of iron powder, Acta Mater. 239 (2022) 118261, https://doi.org/10.1016/J.ACTAMAT.2022.118261.
[11] M. Baigmohammadi, W. Prasidha, N.C. Stevens, Y.L. Shoshyn, T. Spee, P. de Goey, Towards utilization of iron powders for heating and power, Appl. Energy Combust. Sci. 13 (2023) 100116, https://doi.org/10.1016/J.JAECS.2023.100116.
[12] W. Prasidha, M. Baigmohammadi, Y. Shoshin, P. de Goey, Towards an efficient metal energy carrier for zero–emission heating and power: iron powder combustion, Combust. Flame 268 (2024) 113655, https://doi.org/10.1016/J.COMBUSTFLAME.2024.113655.
[13] H. Wiinikka, T. Vikström, J. Wennebro, P. Toth, A. Sepman, Pulverized sponge iron, a zero-carbon and clean substitute for fossil coal in energy applications, Energy Fuel 32 (2018) 9982–9989, https://doi.org/10.1021/ACS.ENERGYFUELS.8B02270/ASSET/IMAGES/LARGE/EF-2018-022704_0006.JPEG.
[14] G. Sun, B. Li, H. Guo, W. Yang, S. Li, J. Guo, Thermodynamic study on reduction of iron oxides by H2 + CO + CH4 + N2 mixture at 900 °C, Energies 13 (2020) 5053, https://doi.org/10.3390/en13195053.
[15] A. Fabozzi, F. Cerciello, O. Senneca, Reduction of iron oxides for CO2 capture materials, Energies 17 (2024) 1673, https://doi.org/10.3390/en17071673.
[16] D. Spreitzer, J. Schenk, Reduction of iron oxides with hydrogen—a review, Steel Res. Int. 90 (2019) 1900108, https://doi.org/10.1002/srin.201900108.
[17] A. Pineau, N. Kanari, I. Gaballah, Kinetics of reduction of iron oxides by H2: Part I: low temperature reduction of hematite, Thermochim. Acta 447 (2006) 89–100, https://doi.org/10.1016/J.TCA.2005.10.004.
[18] C.J.M. Hessels, T.A.M. Homan, N.G. Deen, Y. Tang, Reduction kinetics of combusted iron powder using hydrogen, Powder Technol. 407 (2022) 117540, https://doi.org/10.1016/J.POWTEC.2022.117540.
[19] F. Cerciello, A. Fabozzi, C. Yannakis, S. Schmitt, O. Narin, V. Scherer, et al., Kinetics of iron reduction upon reduction/oxidation cycles, Int. J. Hydrogen Energy 65 (2024) 337–347, https://doi.org/10.1016/J.IJHYDENE.2024.04.008.
[20] N.C. Stevens, W. Prasidha, N.G. Deen, L. Meeuwsen, M. Baigmohammadi, Y. Shoshin, et al., Cyclic reduction of combusted iron powder: a study on the material properties and conversion reaction in the iron fuel cycle, Powder Technol. 441 (2024) 119786, https://doi.org/10.1016/J.POWTEC.2024.119786.
[21] C. Kuhn, A. Düll, P. Rohlfs, S. Tischer, M. Börnhorst, O. Deutschmann, Iron as recyclable energy carrier: feasibility study and kinetic analysis of iron oxide reduction, Appl. Energy Combust. Sci. 12 (2022) 100096, https://doi.org/10.1016/J.JAECS.2022.100096.
[22] Y. Lara, P. Lisbona, A. Martínez, L.M. Romeo, A systematic approach for high temperature looping cycles integration, Fuel 127 (2014), https://doi.org/10.1016/j.fuel.2013.09.062.
[23] S. Pascual, P. Lisbona, L.M. Romeo, Operation maps in calcium looping thermochemical energy storage for concentrating solar power plants, J. Energy Storage 55 (2022) 105771, https://doi.org/10.1016/J.EST.2022.105771.
[24] Eindhoven University of Technology, TU/e demonstrates iron fuel at brewery Bavaria: a new circular and CO2-free fuel for the industry. Eindhoven Univ. Technol. 2020. https://www.tue.nl/en/news-and-events/news-overview/29-10-2020-tue-demonstrates-iron-fuel-at-brewery-bavaria-a-new-circular-and-co2-free-fuel-for-the-industry/#top.
[25] E. Ackerman, Iron Powder Passes First Industrial Test as Renewable, Carbon Dioxide-Free Fuel. IEEE Spectr 2020. https://spectrum.ieee.org/iron-powder-passes-first-industrial-test-as-renewable-co2free-fuel.
[26] RIFT Development B.V. Iron Fuel Technology™. Iron Fuel Technol 2023. https://www.ironfueltechnology.com/technology/.
[27] L. Romeo, C. Mayoral, S. Jiménez, B. Rubio, J. Andrés, Energy storage using direct iron oxide reduction and energy utilization with high temperature metal combustion. Proc. INFUB-14, Algarve, Portugal: 2024.

[28] S. Jiménez, M.C. Mayoral, L.M. Romeo, Detailed physicochemical evolution of iron particles burnt under controlled, realistic conditions, Fuel 391 (2025) 134668, https://doi.org/10.1016/J.FUEL.2025.134668.
[29] J. Neumann, Q. Fradet, A. Scholtissek, F. Dammel, U. Riedel, A. Dreizler, et al., Thermodynamic assessment of an iron-based circular energy economy for carbon-free power supply, Appl. Energy 368 (2024) 123476, https://doi.org/10.1016/J.APENERGY.2024.123476.
[30] International Renewable Energy Agency. Green Hydrogen Cost Reduction: Scaling up Electrolysers to Meet The 1.5°C Climate Goal H 2020.
[31] L.M. Romeo, S. Espatolero, I. Bolea, Designing a supercritical steam cycle to integrate the energy requirements of CO2 amine scrubbing, Int. J. Greenh. Gas Control 2 (2008) 563–570, https://doi.org/10.1016/j.ijggc.2008.03.002.
[32] A.I. Escudero, S. Espatolero, L.M. Romeo, Y. Lara, C. Paufique, A.L. Lesort, et al., Minimization of CO2capture energy penalty in second generation oxy-fuel power plants, Appl. Therm. Eng. 103 (2016) 274–281, https://doi.org/10.1016/j.applthermaleng.2016.04.116.
[33] J.O. Jensen, A.P. Vestbø, Q. Li, N.J. Bjerrum, The energy efficiency of onboard hydrogen storage, J. Alloy. Compd. 446–447 (2007) 723–728, https://doi.org/10.1016/J.JALLCOM.2007.04.051.